

Supplementary Material for the role of conductivity discontinuities in design of cardiac defibrillation

Hyunkyung Lim,¹ Wenjing Cun,¹ Yue Wang,¹ Richard A. Gray,² and James Glimm¹

¹*Department of Applied Mathematics and Statistics, Stony Brook University,
Stony Brook, NY 11794-3600, USA*

²*Center for Devices and Radiological Health, Food and Drug Administration,
Silver Spring, MD 20993-0002, USA*

I. METHODS

We propose eight software developments to be used in conjunction with electrocardiac packages.

1. We add an electroporation current to the ionic currents, needed in the presence of the extreme voltages from the external electrical shock¹⁻³.
2. We use and develop data cleaning tools. These are not needed for the study of the rabbit, but were used for the rat and will be needed for study of new experimentally derived data sets.
3. We introduce an algorithm to identify the individual blood vessels from among the finite element boundaries already identified as tissue surface triangles. These blood vessel triangles form the surface of a blood vessel, which we interpret as an inner surface. The blood vessels of the rabbit, with the cardiac surface removed, are obtained with this algorithm.
4. We add a blood vessel wall outside the specified inner radius by reassigning conductivities for a specified distance from the blood vessel wall. See⁴, especially Fig. 1c. In the region between the inner and outer surfaces of the vessel walls blood vessel wall is added, having its own conductivity.
5. We divide region usually called the bath, the nonheart, nonblood vessel wall region into two distinct components: blood and bath proper (representing pericardial fluid about the heart or the experimental medium in which the isolated heart is located). In other words, the blood and the remainder, nonblood portion of the bath are allowed distinct electrical conductances.
6. We introduce an algorithm that appears to be new for the construction of outer blood vessel walls (not used for the rat heart data).
7. We construct a new finite element volume mesh to adapt to the new surface mesh coming from the outer surface of the blood vessels.

8. A standard construction⁵ allows the construction of fiber orientation from the specification of the cardiac surfaces. We developed a code to generate the fiber orientation consistent with the outer blood vessel wall. The algorithm is described in ref.⁵.

The less obvious developments, steps 2, 3, 6, 7 above are explained in more detail.

- 2* For the rat geometry, data cleaning of the triangulated cardiac surface, downloaded from the website <https://3dprint.nih.gov/discover/3dpx-001642>, was required. We found intersecting triangles and nonmanifold geometry in the triangles describing the rat vasculature. Both were removed with the help of the software package meshlab, <http://www.meshlab.net/>

- 3* To extract the blood vessel surface only from the Chaste rabbit mesh, we introduced an upper surface where the ventricular data has been cut. With this surface included, the blood vessels and the inner and outer heart chamber walls are topologically distinct. These topologically distinct components are isolated using meshlab. The largest components are the interior and exterior of the heart. Of the remainder, we identify as blood vessel fragments any connected surface with an extreme aspect ratio. Visual inspection suggests that most but not all of the small nonheart regions are actually under resolved portions of additional blood vessels. One disconnected region is identified as part of the right ventricle, incorrectly isolated from it.

- 6* When blood vessels are identified by injection of opaque fluid into the blood stream, the result is an identification of the inner blood vessel wall. In this case a further algorithm is needed to specify the outer vessel wall.

Construction of an outer blood vessel outer wall starts with the determination of a smooth normal to the inner surface and of the vessel radius, both defined through meshlab. The wall thickness comes from^{4,6}. The outer blood vessel wall surface is constructed as the solution of a dynamic equation

$$\frac{dx(t)}{dt} = -\mathbf{n} \quad (1)$$

to “grow” the inner surface in the direction $-\mathbf{n}$. \mathbf{n} is oriented outward relative to the cardiac tissue and so $-\mathbf{n}$ is outward relative to the blood vessel. $x(0)$ is some node of a triangle on the inner blood vessel wall, as initial conditions for (1), and the final time for

this equation is set by the wall thickness. At branching points, where the veins divide, the inner surface is concave and the outward dynamics is unstable, leading to self intersections. Conceptually, locations generating self intersections are characterized sharp surface angles and vertices or small triangles. The self intersections are resolved as a manual smoothing operation by relocating a few bad points of the outward growing surface. The blood vessel wall has sufficient thickness that the construction will not add appreciably to the mesh size.

As in ref.⁷, we estimate a relevant blood vessel radius⁴ based on the experimental blood vessel wall thickness as used in ref.⁶. We note a possible experimental uncertainty regarding the blood vessel wall thickness, in that the canine experimental value⁸, the human data⁶ and value used for rabbit simulation do not coincide. Fortunately, the simulations are not particularly sensitive to this parameter.

The blood vessel arterial wall thickness $l = 3.87a^{0.63}$ depends on the outer vessel radius a , with l and a in microns^{4,6}. The analysis of small blood arteries (50 microns outer radius) involves an extrapolation of the data beyond the range reported in ref.⁹i, for which ref.¹⁰ is used; The same ref.¹⁰ offers a formula for the wall thickness of veins.

7* The mesh generation starts with the surfaces which are defined by the blood vessel wall and the heart tissue surfaces from the Chaste rabbit mesh. After constructing the surface mesh with above specified boundaries, we construct the volume mesh using the software tetgen. This software will respect the prescribed surface and avoid small tets, but it is not suitable for finite element simulation, as it typically contains tets with bad aspect ratios. We detected the problem tets as falling into two classes: nearly planar tets, with one very small altitude, and nearly linear tets, with one very small surface triangle. We constructed an algorithm and a software implementation to detect which problem a given bad aspect ratio tet has. In each case we solve a localized mesh optimization problem using the software NLOpt to move tet mesh points subject to the constraint that no moving tet point crosses the surface of some other tet. For the bad tri case, the tri cannot be a surface tri (as this problem is solved in the surface generation stage), so movement of the other tet vertices will not affect the input surface. For the small altitude case, the bad tet mesh point could be on the surface. If so, rather than move a surface point, the optimization moves (typically)

three non-surface points for its optimization.

II. COMPUTING ENVIRONMENT

All simulations were performed on the Handy cluster at Stony Brook University. This hardware includes 40 compute nodes (each with dual socket 2.6 GHz Xeon E5-2670 processors, 16 cores per node, and 128 GB of memory), and two high-performance file servers direct attached to a total of 350 TB of storage.

Typical simulations used 144 cores, and for 10 ms of simulation time required 5 hours.

III. ADDITIONAL SIMULATIONS

A. Time sequence of 3D simulations shown in a slice

We present complete time sequences for the simulation of weak shocks at 3 values of the blood vessel wall conductivities (0.01, 0.2, 1.0 S/m), showing a 2D slice from the 3D simulation from 1 to 9 ms in increments of 1 ms. We also present the time sequence 1 to 4 ms for the rat simulation, strong and weak shocks of isotropic model.

B. Slab simulations and a minimum radius for blood vessels

1. *Prior slab studies*

We discuss results from refs.^{4,7,11,12}. In the high dimensional space of model parameters (vessel type, i.e. artery or vein, vessel wall model or not, vessel radius, shock voltage strength initial conditions, and make or break waves), we and other authors select a few parameters for systematic variation while holding others fixed. Over all conclusions from this body of work are consistent, that the blood vessel walls matter, that the recommended voltages of Ref.¹³ may be less effective than claimed, or for reasons other than claimed, and that the results from simulation studies offer greater precision than qualitative conclusions from scaling laws. Ref.¹¹ holds fixed the vessel radii (considering only two sizes, large and small, and only arteries), while varying the shock strength and the initial conditions, in a systematic study in a slab geometry. Ref.¹² presents analytical methodology and supporting

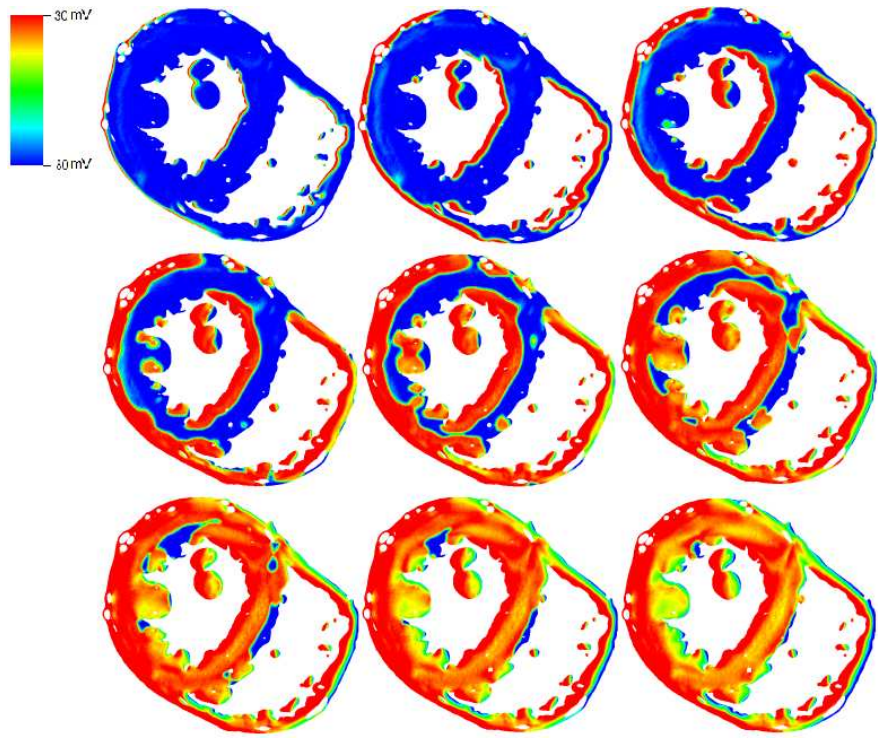


FIG. 1. Weak shock, vessel wall conductance 0.01

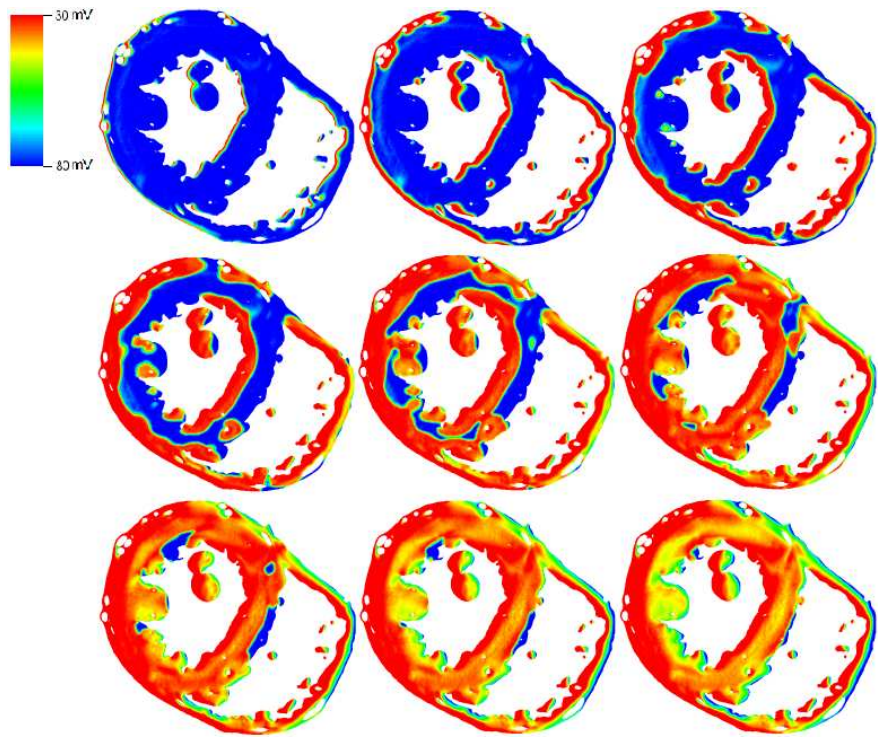


FIG. 2. Weak shock, vessel wall conductance 0.20

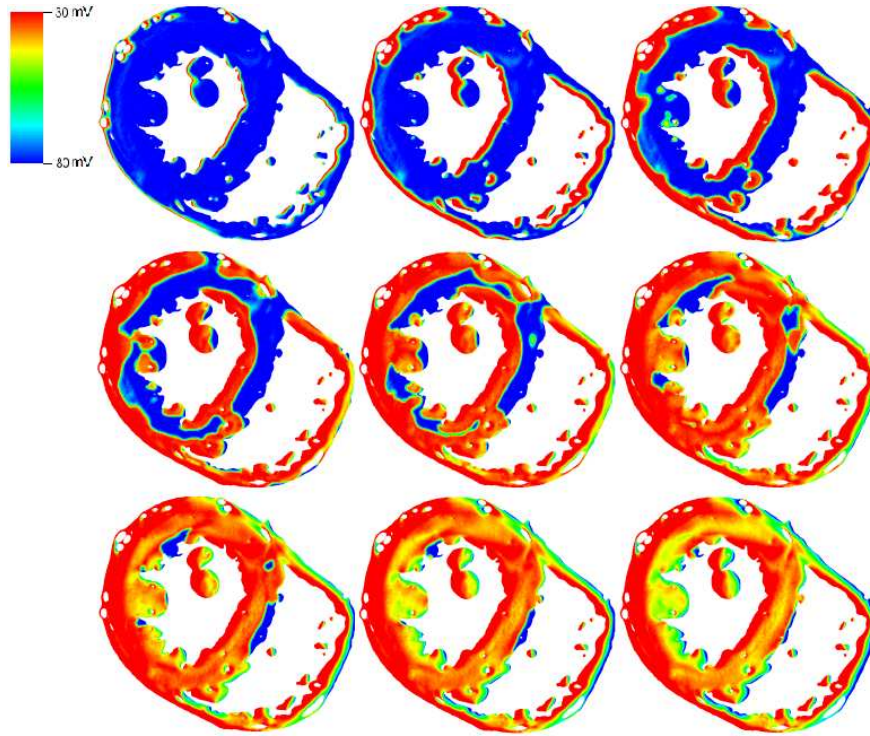


FIG. 3. Weak shock, vessel wall conductance 1.0

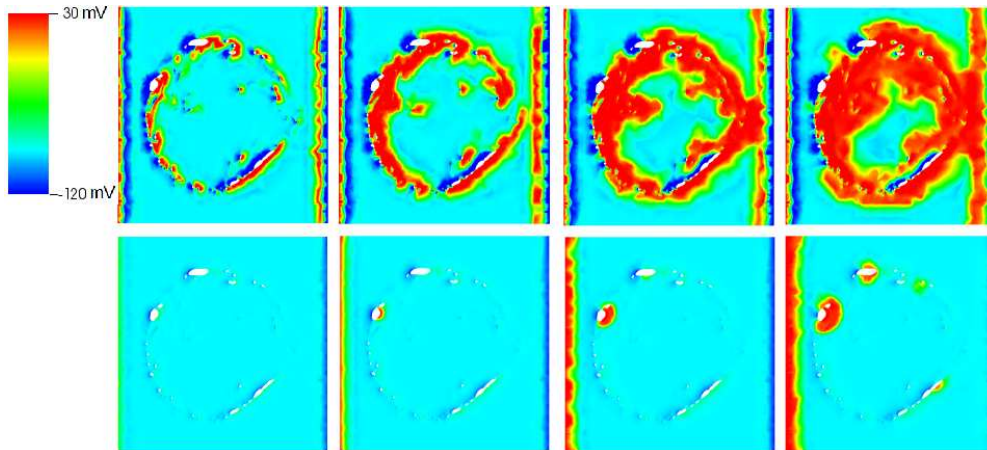


FIG. 4. Rat vasculature isotropic simulations, showing the evolution from 1 to 4 ms in increments of 1 ms. Above: strong shock, Below: weak shock, vessel wall conductance 1.0

simulations study the roles played by endocardial grooves and arterial blood vessels with and without walls (of large and small size). Ref.^{4,7} study minimum shock strength in slab models as a function of the vessel (inner) radius. Here the focus is on break waves, in contrast to our study of make waves. The results are qualitatively similar, but with larger

shock strengths and minimum radii than we find. Our results map out different regions of the high dimensional parameter space than other studies, with the reduced variation of parameters a necessity even for the very simplified slab models. Our main point, consistent with the prior work of others, is that scaling law estimates are imprecise or misleading in their predictions, perhaps due to unquantified parameters or coefficients multiplying the scaling power law. As we vary the parameters we have selected for study, the result in terms of a minimum radius for formation of a make wave can vary by factors of at least 2 or 4. When this uncertainty is mapped onto a density of blood vessels, the resulting availability of blood vessels to initiate defibrillating wave fronts is subject to significant change.

2. Methods

For each of the $6 = 3 \times 2$ cases of blood vessel type and fiber orientation, we present detailed simulation studies to justify the choice of a minimum radius for the blood vessel to generate a meaningful make wave. The slab is $1500 \times 1000 \times 400$ micron³, with the electric field oriented in the long direction and the blood vessel passing through the short direction. The fibers are oriented either parallel or perpendicular to the electric field gradient. For each of the 6 cases, we consider two radii, the larger with a significant response (or at 400 microns if no response at this size) and the smaller without a significant response. For the considered initial conditions (favorable for the creation of make waves), a 4 V/cm shock is applied for 9 ms to blood vessels of varied sizes in a slab geometry. The choice of 4 V/cm results from an effective voltage drop across cardiac walls if a voltage of 3 V/cm is applied across the full heart.

3. Results

The main criterion for significance is whether the response is growing and to a size large enough affect the advancing make wave front coming from the slab end. For each of the two radii, we show the transmembrane voltage in a color plot at 9 ms. For a more quantitative analysis, we plot the transmembrane voltage along the centerline, comparing all 4 cases in one figure.

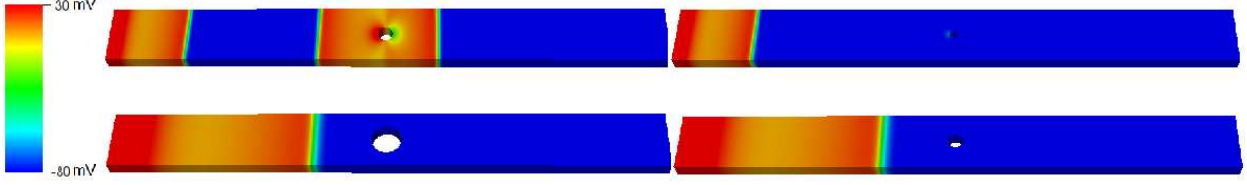


FIG. 5. Transmembrane voltage color plots for arteries. Fibers perpendicular to field gradient (above), parallel (below). Large blood vessel (left), small (right). The large vessel is 400 microns outer radius except for the perpendicular case (then 200 microns), and the small blood vessel is $\times 2$ smaller.

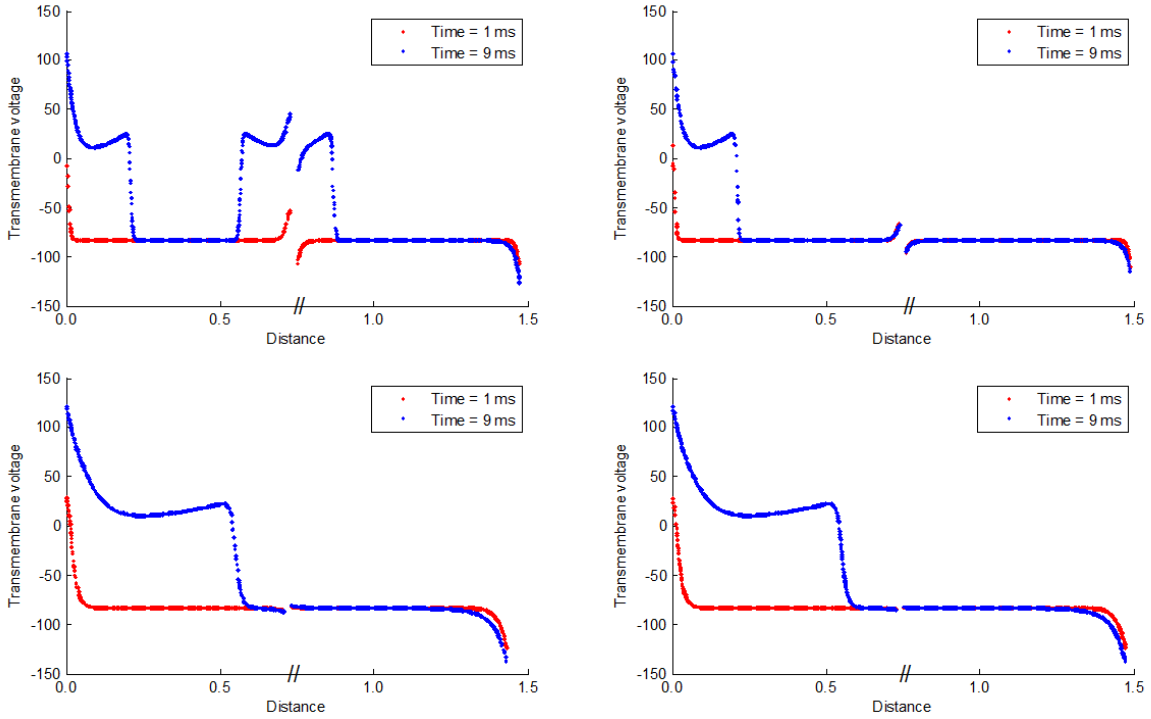


FIG. 6. Transmembrane voltage on a centerline through the slab, at 1 and 9 ms after the electric shock. Fibers perpendicular to field gradient (above), parallel (below). Large blood vessel (right), small (left). The large vessel is 400 microns outer radius except for the perpendicular case (then 200 microns), and the small blood vessel is $\times 2$ smaller.

4. Conclusions

The main conclusion from this slab study is the determination of a minimum radius for the generation of a make wave. This minimum radius is sensitive to the blood vessel type

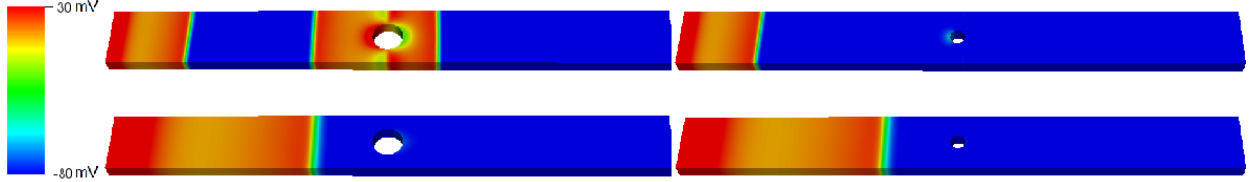


FIG. 7. Transmembrane voltage color plots for veins. Fibers perpendicular to field gradient (above), parallel (below). Large blood vessel (left), small (right). The large vessel is 400 microns outer radius. and the small blood vessel is $\times 2$ smaller.

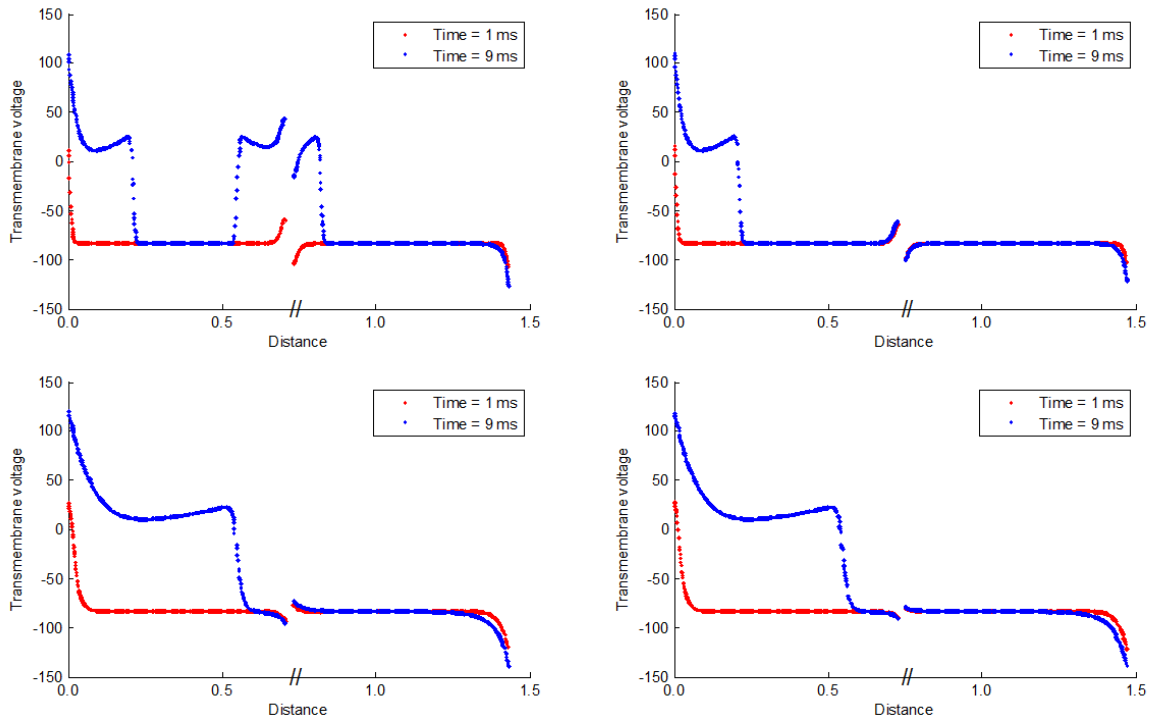


FIG. 8. Transmembrane voltage on a centerline through the slab, at 1 and 9 ms after the electric shock. Fibers perpendicular to field gradient (above), parallel (below). Large blood vessel (left), small (right). The large vessel is 400 microns outer radius. and the small blood vessel is $\times 2$ smaller.

(vein, artery or lacking a wall), and to the orientation of the fibers relative to the electric field gradient. The radius ranges from 200 micron outer radius to at least 800 microns, with the latter case included implicitly is a consequence of a lack of response from a 400 micron radius blood vessel. The resulting minimum radii are tabulated in the journal paper.

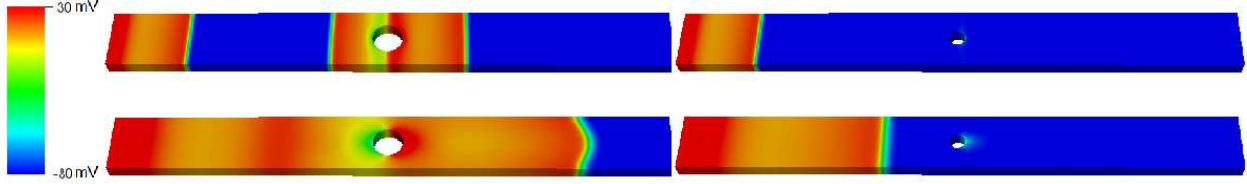


FIG. 9. Transmembrane voltage color plots for vessels with no walls. Fibers perpendicular to field gradient (above), parallel (below). Large blood vessel (right), small (left). The large vessel is 400 microns outer radius. and the small blood vessel is $\times 2$ smaller.

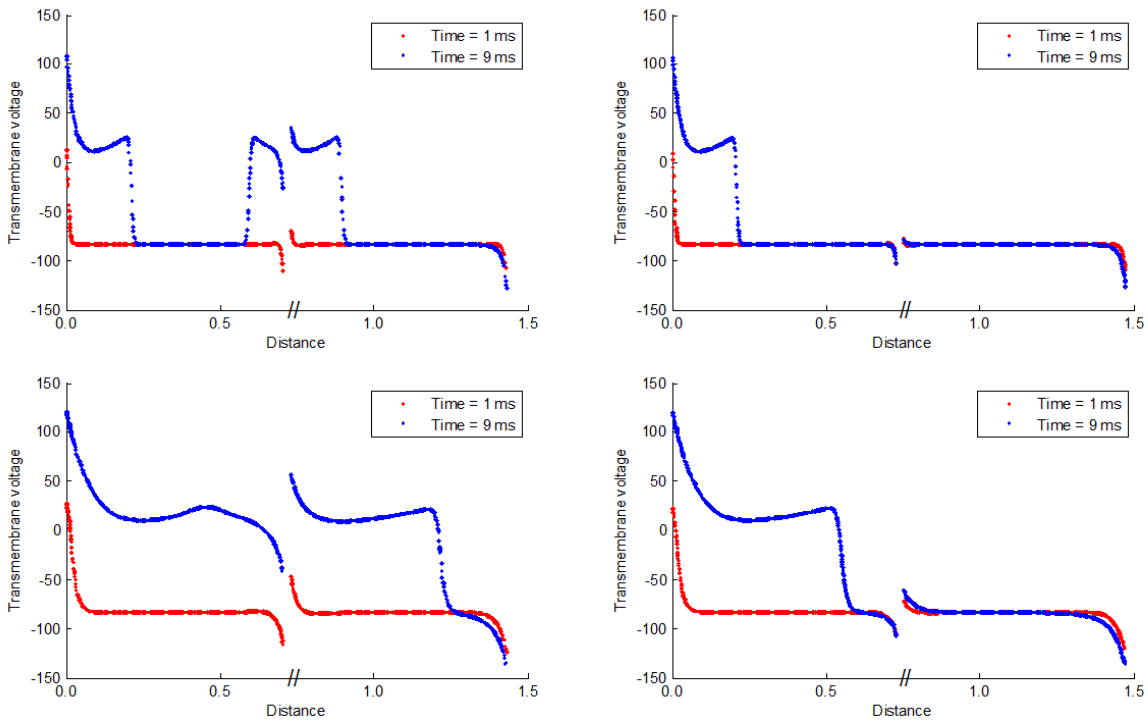


FIG. 10. Transmembrane voltage on a centerline through the slab, at 1 and 9 ms after the electric shock. Fibers perpendicular to field gradient (above), parallel (below). Large blood vessel (right), small (left). The large vessel is 400 microns outer radius. and the small blood vessel is $\times 2$ smaller.

REFERENCES

- ¹W. Krassowska, Pacing and Clinical Electrophysiology **18**, 1644 (1995).
- ²D. K. Cheng, L. Tung, and E. A. Sobie, American Journal of Physiology - Heart and Circulatory Physiology **277**, H351 (1999).
- ³T. Ashihara and N. A. Trayanova, Biophysical Journal **87**, 2271 (2004).

- ⁴M. Bishop, P. M. Boyle, G. Plank, D. G. Walsh, and E. Vigmond, *IEEE Transactions on Biomedical Engineering* **10**, 2335 (2010).
- ⁵J. D. Bayer, R. C. Blake, G. Plank, and N. A. Trayanova, *Ann Biomed Eng.* **40**, 2243 (2012).
- ⁶B. K. Podesser, F. Neumann, M. Neumann, W. Schreiner, G. Wollenek, and R. Mallinger, *Acta Anatomica: Cells, Tissues, Organs* **163**, 63 (1998).
- ⁷M. J. Bishop, G. Plank, and E. Vigmond, *Circulation: Arrhythmia and Electrophysiology* **5**, 210 (2012).
- ⁸R. J. Tomanek, R. J. Palmer, G. I. Peiffer, K. L. Schreiber, C. L. Eastha, and M. L. Marcus, *Circulation Research* **58** (1986).
- ⁹K. R. Visser, *Proceedings of the Annual Conference of the IEEE Engineering* **5**, 1540 (1989).
- ¹⁰A. C. Burton, *Physiol Rev.* **34**, 619 (1954).
- ¹¹A. Connolly, E. Vigmond, and M. Bishop, *Front Bioeng Biotechnol.* **5** (2017).
- ¹²A. Connolly, E. Vigmond, and M. Bishop, *PLoS One* **12**, e0173324 (2017).
- ¹³S. Luther, F. H. Fenton, B. G. Kornreich, A. Squires, P. Bittihn, D. Hornung, and M. Z. et al, *Nature* **475**, 235 (2011).